UCLA
COMPUTATIONAL AND APPLIED MATHEMATICS

Towards An Hybrid Monte Carlo Method for Rarefied Gas Dynamics

Russel E. Caflisch
Lorenzo Pareschi

December 2000
CAM Report 00-44

Department of Mathematics
University of California, Los Angeles
Los Angeles, CA. 90095-1555

http://www.math.ucla.edu/applied/cam/index.html

TOWARDS AN HYBRID MONTE CARLO METHOD FOR RAREFIED GAS DYNAMICS

RUSSEL E. CAFLISCH* AND LORENZO PARESCHI†

Abstract. For the Boltzmann equation, we present an hybrid Monte Carlo method that is robust in the fluid dynamic limit. The method is based on representing the solution as a convex combination of a non-equilibrium particle distribution and a Maxwellian. The hybrid distribution is then evolved by Monte Carlo with an unconditionally stable and asymptotic preserving time discretization. Some computational simulations of spatially homogeneous problems are presented here and extensions to space non homogeneous situations discussed.

Key words. Boltzmann equation, fluid dynamic limit, Direct Simulation Monte Carlo

AMS(MOS) subject classifications.

1. Introduction.

2. The Boltzmann equation.

We consider the initial boundary value problem for the Boltzmann equation [3]

$$\frac{\partial f}{\partial t} + v \cdot \nabla_x f = \frac{1}{\varepsilon} Q(f,f), \quad v \in I\!R^3,\ x \in \Omega \subset I\!R^3, \tag{2.1}$$

$$f(x,v,t=0) = f_0(x,v), \tag{2.2}$$

$$|v\cdot n| f(x,v,t) = \int_{v_*\cdot n<0} |v_*\cdot n(x)| K(v_* \to v, x, t) f(x, v_*, t)\, dv_* \text{ for } v\cdot n \geq 0, x \in \partial\Omega. \tag{2.3}$$

In (2.1) $f = f(x,v,t)$ is a non negative function describing the time evolution of the distribution of particles which move with velocity $v \in I\!R^3$ in position $x \in I\!R^3$ at time $t > 0$. The smooth boundary $\partial\Omega$ is assumed to have a unit inner normal $n(x)$ at every $x \in \partial\Omega$.

The parameter $\varepsilon > 0$ is called the Knudsen number and is proportional to the mean free path between collisions. The bilinear collision operator $Q(f,f)$, which describes the binary collisions of the particles, acts on the velocity only and is given by

$$Q(f,f)(v) = \int_{I\!R^3} \int_{S^2} \sigma(|v - v_1|, \omega)[f(v')f(v'_*) - f(v)f(v_*)]\, d\omega\, dv_*. \tag{2.4}$$

In the above expression, ω is a unit vector of the sphere S^2, so that $d\omega$ is an element of area of the surface of the unit sphere S^2 in $I\!R^3$. Moreover (v', v'_*)

* Mathematics Department, UCLA. Email: caflisch@math.ucla.edu. Research supported in part by the NSF through grants number DMS-9623087 and INT-9512772

† Mathematics Department, University of Ferrara. Email: pareschi@dm.unife.it.

represent the pre-collisional velocities associated with the post-collisional velocities (v, v_*) and the collision parameter ω

$$v' = \frac{1}{2}(v + v_* + |v - v_*|\omega), \quad v'_* = \frac{1}{2}(v + v_* - |v - v_*|\omega). \tag{2.5}$$

The kernel σ is a nonnegative function which characterizes the details of the binary interactions. In the case of inverse k-th power forces between particles the kernel has the form

$$\sigma(|v - v_*|, \theta) = b_\alpha(\theta)|v - v_*|^\alpha, \tag{2.6}$$

where $\alpha = (k-5)/(k-1)$. For numerical purposes, a widely used model is the Variable Hard Sphere(VHS) model [1], corresponding to $b_\alpha(\theta) = C_\alpha$ where C_α is a positive constant. The case $\alpha = 0$ is referred to as Maxwellian gas whereas the case $\alpha = 1$ yields the Hard Sphere gas.

2.1. Boundary conditions. The boundary condition (2.3) is the so-called reflective condition on $\partial\Omega$. The ingoing flux is defined in terms of the outgoing flux modified by a given boundary kernel K according to the integral in (2.3). This boundary kernel is such that positivity and mass conservation at the boundaries are guaranteed

$$K(v_* \to v, x, t) \geq 0, \qquad \int_{v \cdot n(x) \geq 0} K(v_* \to v, x, t)\, dv = 1. \tag{2.7}$$

From a physical point of view, we assume that at the solid boundary a fraction α of molecules is absorbed by the wall and then re-emitted with the velocities corresponding to those in a still gas at the temperature of the solid wall, while the remaining portion $(1 - \alpha)$ is perfectly reflected. This is equivalent to impose for the ingoing velocities

$$f(x, v, t) = (1 - \alpha)Rf(x, v, t) + \alpha Mf(x, v, t), \quad x \in \partial\Omega, \quad v \cdot n(x) \geq 0, \tag{2.8}$$

where α, with $0 \leq \alpha \leq 1$, is called the *accomodation coefficient* and

$$Rf(x, v, t) = f(x, v - 2n(n \cdot v), t), \tag{2.9}$$

$$Mf(x, v, t) = \mu(x, t) f_s(v). \tag{2.10}$$

In (2.10), if we denote by T_s the temperature of the solid boundary, f_s is given by

$$f_s(v) = \exp(-\frac{v^2}{2T_s}),$$

and the value of μ is determined by mass conservation at the surface of the wall

$$\mu(x, t) \int_{v \cdot n \geq 0} f_s(v)|v \cdot n| dv = \int_{v \cdot n < 0} f(x, v, t)|v \cdot n| dv. \tag{2.11}$$

We note that according to (2.8), for $\alpha = 0$ (specular reflection) the re-emitted molecules have the same flow of mass, temperature and tangential momentum of the incoming molecules, while for $\alpha = 1$ (full accomodation) the re-emitted molecules have completely lost memory of the incoming molecules, except for conservation of the number of molecules.

2.2. Fluid-dynamical limit. During the evolution process, the collision operator preserves mass, momentum and energy, i.e.,

$$\int_{\mathbb{R}^3} Q(f,f)\phi(v)\,dv = 0, \quad \phi(v) = 1, v, v^2, \tag{2.12}$$

and in addition it satisfies Boltzmann's well-known H-theorem

$$\int_{\mathbb{R}^3} Q(f,f)\log(f)dv \leq 0. \tag{2.13}$$

From a physical point of view, Boltzmann's H-theorem implies that any equilibrium distribution function, i.e. any function f for which $Q(f,f) = 0$, has the form of a locally Maxwellian distribution

$$M(\rho,u,T)(v) = \frac{\rho}{(2\pi T)^{3/2}} \exp\left(-\frac{|u-v|^2}{2T}\right), \tag{2.14}$$

where ρ, u, T are the density, mean velocity and temperature of the gas defined by

$$\rho = \int_{\mathbb{R}^3} f\,dv, \qquad u = \frac{1}{\rho}\int_{\mathbb{R}^3} vf\,dv, \qquad T = \frac{1}{3\rho}\int_{\mathbb{R}^3} [v-u]^2 f\,dv. \tag{2.15}$$

As $\varepsilon \to 0$ the distribution function approaches the local Maxwellian (2.14). In this case the higher order moments of the distribution f can be computed as function of ρ, u, and T, by using (2.14) and we obtain to the leading order the closed system of *compressible Euler equations* of gas dynamics

$$\begin{aligned} &\frac{\partial \rho}{\partial t} + \nabla_x \cdot (\rho u) = 0 \\ &\frac{\partial \rho u}{\partial t} + \nabla_x \cdot (\rho u \otimes u) + \nabla_x p = 0 \\ &\frac{\partial E}{\partial t} + \nabla_x \cdot (Eu + pu) = 0 \end{aligned} \tag{2.16}$$

$$p = \rho T, \quad E = \frac{3}{2}\rho T + \frac{1}{2}\rho u^2. \tag{2.17}$$

3. Time discretizations. A simple splitting of the time scales in (2.1) consists in solving separately a free transport equation

$$\frac{\partial f}{\partial t} + v \cdot \nabla_x f = 0, \tag{3.1}$$

and a space homogeneous problem

$$\frac{\partial f}{\partial t} = \frac{1}{\varepsilon} Q(f,f). \tag{3.2}$$

A general idea for deriving robust numerical schemes, by which we mean schemes that are unconditionally stable and preserve the asymptotics of the fluid dynamic limit of (2.1), is to use suitable implicit time discretizations for the stiff problem (3.2). In fact if a scheme is able to treat the collision step (3.2) for vanishingly small values of ε, then the splitting scheme will become a first order *kinetic scheme* for the underlying fluid dynamic limit.

For a nonlinear equation like (3.2) this is a challenging problem since implicit schemes imply the solution of large systems of nonlinear integral equations which will lead to a prohibitively expensive computational cost.

3.1. Time relaxed (TR) schemes. The schemes presented in [4] are based on the idea to replace high order terms of a suitable well-posed power series expansion of the solution to (3.2) by the local equilibrium (2.14). The great advantage of these schemes is to be unconditionally stable and explicitely implementable.

To this aim, we will assume that the collision kernel satisfies a cut-off hypothesis.

Denote $Q_\Sigma(f,f)$ to be the collision operator obtained by replacing the kernel σ with the kernel σ_Σ

$$\sigma_\Sigma(|v-v_*|,\omega) = \min\left\{\sigma(|v-v_*|,\omega), \Sigma\right\}, \quad \Sigma > 0.$$

Thus, for a fixed Σ, we consider the homogeneous problem

$$\frac{\partial f}{\partial t} = \frac{1}{\varepsilon} Q_\Sigma(f,f). \tag{3.3}$$

Problem (3.3) can be written in the form

$$\frac{\partial f}{\partial t} = \frac{1}{\varepsilon}\left[P(f,f) - \mu f\right] \tag{3.4}$$

taking

$$P(f,f) = Q_\Sigma^+(f,f) + f(v)\int_{\mathbb{R}^3}\int_{S^2}[\Sigma - \sigma_\Sigma(|v-v_*|,\omega)]f(v_*)\,d\omega\,dv_*, \tag{3.5}$$

with $\mu = 4\pi\Sigma\rho$ and

$$Q_\Sigma^+(f,f,) = \int_{\mathbb{R}^3}\int_{S^2}\sigma_\Sigma(|v-v_*|,\omega)f(v')f(v'_*)\,d\omega\,dv_*. \tag{3.6}$$

We can obtain the following formal representation of the solution to the Cauchy problem (3.4)

$$f(v,t) = e^{-\mu t/\varepsilon}\sum_{k=0}^{\infty}\left(1-e^{-\mu t/\varepsilon}\right)^k f_k(v), \tag{3.7}$$

where the functions f_k are given by the formula

$$f_{k+1}(v) = \frac{1}{k+1}\sum_{h=0}^{k}\frac{1}{\mu}P(f_h, f_{k-h}), \quad k = 0, 1, \ldots \tag{3.8}$$

A class of numerical schemes, hereafter called time relaxed (TR) schemes, based on truncating the previous expansion in a small interval Δt taking $f_k = M$ for $k \geq m+1$ with $m \geq 1$ has been proposed in [4].

These schemes have the following properties [4]:

- they are well defined for any value of $\mu\Delta t/\varepsilon$,
- they have the correct moments (since every f_k has the same mass, momentum and temperature of f),
- they are at least a m-order approximation (in $\mu\Delta t/\varepsilon$) of (3.7),
- they will preserve the positivity of the solution,
- for any $m \geq 1$, we have

$$\lim_{\varepsilon/(\mu\Delta t)\to 0} f^{n+1}(v) = M(v).$$

The last property implies the convergence towards the correct fluid-dynamic limit.

In [5] a better truncation, accuracy-wise, has been introduced which corresponds to take $f_{m+1} = f_m$, $f_k = M$, $k \geq m+2$ in (3.7). Obviously all the previous properties continue to hold also in this case.

Note that since the coefficients $f_k(v)$, $k \geq 1$, of expansion (3.8), include numerous five fold integral like (3.5), the most efficient scheme for practical applications is that for $m = 1$.

This first order TR approximation can generally be written in the form

$$f^{n+1}(v) = A(\lambda)f^n(v) + B(\lambda)f_1^n(v) + C(\lambda)M(v) \tag{3.9}$$

where $\lambda = \mu\Delta t/\varepsilon$ and the weights A, B and C are nonnegative functions that satisfy

$$A(\lambda) + B(\lambda) + C(\lambda) = 1, \quad \forall\lambda. \tag{3.10}$$

The truncation proposed in [5] cooresponds to

$$A = 1 - \tau, \quad B = \tau(1-\tau^2), \quad C = \tau^3. \tag{3.11}$$

4. Hybrid formulation and Monte Carlo methods. In this section, we formulate an analytic representation for the density function f which takes advantage of the relaxed time discretization presented in the previous section. Next the analytic representation will be translated into a numerical representation. Specifically one of the components of f will be replaced by a discrete set of particles.

4.1. Collision step. As derived in the previous section, the general form for a single step of the TR discretization is

$$f^{n+1} = Af^n + Bf_1^n + CM \tag{4.1}$$

in which f^n is the density function at time step n, $f_1^n = P(f^n, f^n)/\mu$ is the first order term in (3.7) and the coefficients A, B, C are positive constants as in the previous section.

In order to analyze and exploit the discretization (4.1), write f as the linear combination of a Maxwellian density and a non-Maxwellian density, as

$$f^n(v) = (1-\beta^n)g^n(v) + \beta^n M(v) \tag{4.2}$$

in which β is a nonnegative scalar. The Maxwellian density M is chosen to have the same mass, momentum and temperature as f^n.

In (4.2) we have omitted the superscript n on M, since ρ, u and T are independent of n during the collision step, and as a result M is independent of n.

Now insert the representation (4.2) for f^n into the discretization (4.1) and use the fact that

$$f_1(M, M) = M. \tag{4.3}$$

The right hand side of (4.1) then naturally splits into a Maxwellian part $\beta^{n+1}M$ and a non-Maxwellian part $(1-\beta^{n+1})g^{n+1}$, in which

$$\begin{aligned} \beta^{n+1} &= A\beta^n + B(\beta^n)^2 + C \qquad (4.4)\\ (1-\beta^{n+1})g^{n+1} &= A(1-\beta^n)g^n + B(1-\beta^n)^2 f_1(g^n, g^n) \\ &\quad + 2B(1-\beta^n)\beta^n f_1(g^n, M). \qquad (4.5) \end{aligned}$$

It follows that for $C \neq 1$

$$g^{n+1} = (A + B(1+\beta^n))^{-1} \left(Ag^n + B(1-\beta^n)f_1(g^n, g^n) + 2B\beta^n f_1(g^n, M)\right). \tag{4.6}$$

Equation (4.4) is an iterated map for the coefficient β and can be rewritten using the conservation property (3.10) as

$$\beta^{n+1} - \beta^n = B(\beta^n - 1)(\beta^n - C/B). \tag{4.7}$$

This discrete dynamical system has stationary points $\beta = 1$ if $C/B > 1$ and $\beta = C/B$ if $C/B < 1$ [2]. Unfortunately the requirement $C/B > 1$ cannot be verified uniformly in $\lambda = \mu\Delta t/\epsilon$. However, the fluid regime corresponds to $\lambda \gg 1$ so that $C/B \gg 1$ because of the asymptotic preserving property. This shows that β^n increases monotonically to 1 in the fluid region, as desired. For example, for the first order scheme corresponding to (3.11)

$C/B = \tau^2/(1-\tau^2)$. Hence $\beta^n \to 1$ if $\tau > 1/\sqrt{2}$. Clearly, near the fluid limit $\mu\Delta t/\varepsilon \gg 1$ and hence $\tau = 1 - e^{-\mu\Delta t/\varepsilon} \approx 1$.

Next we describe our algorithm based on the evolution of the mixed distribution $f = (1-\beta)g + \beta M$. The distinguishing feature of our method is that the Maxwellian part of the distribution is represented analytically and the non Maxwellian fraction is represented as a particle distribution

$$g^n(v) = \frac{1}{N_n}\sum_{i=1}^{N_n}\delta(v - v_i^n). \tag{4.8}$$

Our starting point is the evolution equation (4.5) for g^n, which can be written as

$$g^{n+1} = p_1 g^n + p_2\left[q_1\frac{P(g^n,g^n)}{\mu} + q_2\frac{P(g^n,M)}{\mu}\right], \tag{4.9}$$

in which

$$p_1 = \frac{A}{A + B(1+\beta^n)}, \quad p_2 = \frac{B(1+\beta_n)}{A + B(1+\beta_n)}, \tag{4.10}$$

$$q_1 = \frac{1-\beta^n}{1+\beta^n}, \quad q_2 = \frac{2\beta^n}{1+\beta^n}. \tag{4.11}$$

Note that if f^n is a probability density, so is g^n. Moreover, $p_1 \geq 0$, $p_2 \geq 0$, $p_1 + p_2 = 1$, $q_1 \geq 0$, $q_2 \geq 0$, $q_1 + q_2 = 1$, and therefore p_1 and p_2 can be interpreted as probabilities, and q_1 and q_2 can be interpreted as conditional probabilities.

Therfore, Eq. (4.9) has the following probabilistic interpretation: a particle extracted from g^n has no collision with probability p_1, it collides with another particle extracted from g^n with probability p_2q_1, or it collides with a particle sampled from the Maxwellian with probability p_2q_2.

Note that this probabilistic interpretation is uniformly valid in $\mu\Delta t/\epsilon$. Moreover as $\mu\Delta t/\epsilon \to \infty$, $\beta^n \to 1$ because of the asymptotic preserving property of the quantities A, B and C. Therefore the density function f^n has the correct fluid limit.

REMARK 4.1. If the number of particles is kept fixed, then their weight changes, since the mass associated to the particles is proportional to $(1-\beta^n)$. Instead, we chose to use a variable number of particles with constant weight per particle. This choice has several advantages. It improves the efficiency of the method, since the number of particles (and hence the computational cost) decreases without affecting the accuracy, and it simplifies the exchange of particles between cells in a spatially inhomogeneous problem.

An acceptance-rejection technique, similar to the one used for DSMC, can be adopted to derive a Monte Carlo algorithm. The algorithm to update β^n and g^n starting with N_n particles can be written as

ALGORITHM 4.1. :

1. *set* $\beta^{n+1} = 0, N_c = 0$
2. *compute an upper bound* Σ *of* σ_{ij} *(as in DSMC)*
3. *compute* $\tau = \exp(-\rho\Sigma\Delta t/\epsilon)$ *and the corresponding quantities* p_1, p_2, q_1, q_2
4. *compute the number of dummy collision pairs:*
   - $N_{gM} = p_2 q_2 N_n/2$
   - $N_{gg} = p_2 q_1 N_n/2$
5. *perform* N_{gg} *dummy collisions between g-particles, i.e.*
   - *extract* (i, j) *without repetition*
   - *compute* $\tau_{ij} = \exp(-\rho\sigma_{ij}\Delta t/\epsilon)$ *and the corresponding quantities* A_{ij}, B_{ij}, C_{ij}
   - $\beta_{ij} = A_{ij}\beta^n + B_{ij}(\beta^n)^2 + C_{ij}$
   - *if* $\sigma\,\mathrm{Rand} < \sigma_{ij}$ *then perform the collision between* v_i *and* v_j *(as in standard DSMC)*
     - $\beta^{n+1} \leftarrow \beta^{n+1} + 2\beta_{ij}$
     - $N_c \leftarrow N_c + 2$
6. *perform* $2N_{gM}$ *dummy collisions between the g-particles and the Maxwellian,*
   - *extract* i *without repetition*
   - *sample one particle,* m*, from the Maxwellian*
   - *compute* $\tau_{im} = \exp(-\rho\sigma_{im}\Delta t/\epsilon)$ *and the corresponding quantities* A_{im}, B_{im}, C_{im}
   - $\beta_i m = A_{im}\beta^n + B_{im}(\beta^n)^2 + C_{im}$
   - *if* $\sigma\,\mathrm{Rand} < \sigma_{im}$ *then perform the collision between* v_i *and the Maxwellian*
     - $\beta^{n+1} \leftarrow \beta^{n+1} + \beta_{im}$
     - $N_c \leftarrow N_c + 1$
7. $\beta^{n+1} = \beta^{n+1}/N_c$
8. *update* N*:* $N_{n+1} = \mathrm{Round}(N_n(1 - \beta^{n+1}))$
9. *correct* β^{n+1} *in order to preserve mass*

The above scheme conserves momentum and energy only on the average, but not exactly (except for $\beta^n = 0$). This is because the collisions with the Maxwellian M, if performed independently from each other, do not maintain exact conservation of momentum and energy. By taking this into account, a conservative algorithm can be constructed by modifying the moments associated to the Maxwellian fraction u_M and E_M at the end of each time step.

This is obtained by imposing

$$(1 - \beta^{n+1})E_p + \beta^{n+1}E_M = E^0, \quad (1 - \beta^{n+1})u_p + \beta^{n+1}u_M = u^0, \quad n > 0,$$

where u_p and E_p are the mean velocity and energy of the particles. The previous system can be solved with respect to u_M and E_M if β^n is not too small.

If the distribution is very far from equilibrium, i.e. if $\beta_n \ll 1$, then because of fluctuations, it may happen that the energy decreases too much, and it is impossible to change the parameters of the Maxwellian to impose

conservation. On the other hand, in this case, only a very small fraction of collisions will be non conservative, and therefore the lack of exact conservation will not affect the quality of the result.

4.2. Transport step. Note that in the space homogeneous case, the Maxwellian equilibrium fraction β^{n+1} can only increase, and, consequently, the number of particles can only decrease if we start from a a completely discrete distribution ($\beta^n = 0$). When $N^{n+1} < N^n$, some particles are just disregarded. As we shall discuss in the sequel, convection distorts the Maxwellian, and provides a mechanism for creating new particles.

When the transport step (3.1) is applied in a time interval Δt to a mixed distribution of the general form $f^n(x,v) = (1-\beta^n)g^n(x,v) + \beta^n M^n(x,v)$ (here the superscript n must be kept) we obtain

$$f(x,v,\Delta t) = (1-\beta^n)g^n(x-vt,v) + \beta^n M^n(x-v\Delta t,v). \tag{4.12}$$

The distribution of particles $g^n(x-vt,v)$ can be obtained as in standard Monte Carlo methods by exact free flow. Denoting with x_i^n and v_i^n respectively the positions and the velocities of particles that characterize the distribution g^n after the collision step, the new particles positions are computed accordingly to

$$x_i^* = x_i^n + v_i\Delta t, \qquad i = 1,\cdots,N^n. \tag{4.13}$$

This originates the new particle distribution $\tilde{g}^*(x,v)$ and hence a representation of the solution at the next time level t^* of the form

$$f^*(x,v) = (1-\beta^n)\tilde{g}^*(x,v) + \beta^n M^n(x-v\Delta t,v), \tag{4.14}$$

which should be projected back to an expression like $(1-\beta^*)g^*(x,v) + \beta^* M^*(x,v)$, in order to apply the next collision routine.

A simple way to do this is to set $\beta^* = 0$ and therefore

$$g^*(x,v) = (1-\beta^n)\tilde{g}^*(x,v) + \beta^n M^n(x-v\Delta t,v),$$

by transforming all the analityc distribution function $M^n(x-v\Delta t,v)$ into particles by sampling. If we denote by m_p is the mass of a single particle, by N_p^* the number of particles that characterize $\tilde{g}^*(x,v)$ after free flow and by ρ^* the total mass in the cell computed from (4.14), then setting

$$N^* = \text{Round}\left(\frac{\rho^*}{m_p}\right),$$

we must sample $N_M^* = N^* - N_p^* \geq 0$ particles from $M^n(x-v\Delta t,v)$ and then correct β^* in order to preserve the mass. Unfortunately this creation of particles will not be very efficient, in particular when $\beta^n \approx 1$, i.e. close to the fluid limit. In this case, in fact, at every time step we will discard

almost all particles during the collision step ($N_p^* \approx 0$) and then transform everything back to particles after the transport ($N_M \approx N^*$).

REMARK 4.2. *The same result can be obtained transforming the Maxwellian M^n into a particle distribution (for example using Pullin's algorithm [7] this can be done in a conservative way) at the end of the collision step, similarly to the algorithms developed in [5], [6]. In this way the previous sampling will be equivalent to the free flow of particles sampled from M^n.*

The possibility to obtain numerical algorithms with a better computational efficiency, for example using an estimator of the number of particles that will be discarded during the collision step in order to avoid the generation of too many particles after the transport, is actually under study.

5. Numerical Results. In this section we test the hybrid time relaxed Monte Carlo (TRMCH) by comparing it with standard DSMC. We consider here some preliminary results on space homogeneous problem. In our tests we use the set of parameters defined by (3.11) and perform a single run, with a number of particles sufficiently large to control the effects of the fluctuations. We express the results as a function of the scaled time variable t/ϵ which we denote again by t in order to simplify the notations.

5.1. Maxwell molecules. Next we consider the 2D homogeneous Boltzmann equation for Maxwell molecules. An exact solution of the equation corresponding to the initial condition

$$f_0(v) = \frac{v^2}{\pi} \exp\left(-v^2\right), \tag{5.1}$$

is given by

$$f(v,t) = \frac{1}{2\pi C}\left[1 - \frac{1}{C}(1-C)\left(1 - \frac{v^2}{2C}\right)\right] \exp\left(-\frac{v^2}{2C}\right), \tag{5.2}$$

where $C(t) = 1 - (1/2)\exp(-t/8)$.

The comparison with the exact solution is obtained by reconstructing the function on a regular grid of spacing $\Delta v = 0.25$ by the weighted area rule.

All the simulations have been performed for $t \in [0, 16]$ by starting with $N = 10^5$ particles.

In Fig. 6.1 we show the L^2 norm of the error in time for both DSMC and TRMCH on the time interval [0,8]. In the first test we use the same time step $\Delta t = 0.4$. The results confirm the gain of accuracy of the TRMCH method on the transient time scale (left). For $t \geq 4$, the methods are almost equivalent since the maximum value reached by β^n at the end of the simulation is about 0.12 and hence most of the distribution is composed of particles.

Using a time step of $\Delta t = 0.6$ for the TRMCH and $\Delta t = 0.15$ for the DSMC the gain of accuracy is less evident but more uniform in time (right). Here the final value of β^n is about 0.25.

5.2. VHS molecules. The last test problem deals with the numerical solution of the Boltzmann equation for Hard Sphere molecules (VHS, for $\alpha = 1$) with $C_\alpha = 1$.

The initial condition is the same used for the Maxwell molecules (5.1). The "exact" solution has been computed using the DSMC method with 2×10^6 particles and $\Delta t = 5 \times 10^{-3}$.

As in the previous case, the density distribution is obtained by reconstructing the function on a regular grid of spacing $\Delta v = 0.25$ by the "weighted area rule" and the simulations have been performed for $t \in [0, 16]$ by starting with $N = 10^5$ particles.

In Fig. 6.2 we show the time evolution of the fourth order moment of the solution. The results confirm the gain of accuracy and the reduction of fluctuations of the TRMCH method with respect to the DSMC method for larger time steps.

Next we report the number of dummy collisions and the number of effective collisions per time step performed by DSMC and TRMCH (Fig. 6.3).

In spite of the fact that the time step for TRMCH is larger than that of DSMC, the number of dummy collision is higher for DSMC. The reason is that this number is proportional to $\mu\Delta t$ for DSMC, and it is proportional to $1 - \exp(-\mu\Delta t)$ for TRMCH. This is an additional reason of the better efficiency of the TRMCH with respect to DSMC.

Finally we give in Fig. 6.4 the variations of β^n and of the number of particles in time for the TRMCH method.

6. Conclusion and perspectives.

Acknowledgements. L. Pareschi would like to thanks the Mathematics Department of UCLA for the kind ospitality during the time part of this work was carried out.

REFERENCES

[1] G.A. Bird. *Molecular Gas Dynamics.* Oxford University Press, London, 1976.
[2] R.Caflisch and L. Pareschi. An Implicit Monte Carlo method for rarefied gas dynamics I. The space homogeneous case. *J. Comp. Phys.*, 154, 90–116, 1999.
[3] C. Cercignani. *The Boltzmann Equation and its Applications.* Springer-Verlag, 1988.
[4] E. Gabetta, L. Pareschi, and G. Toscani. Relaxation schemes for nonlinear kinetic equations. *SIAM J. Num. Anal.*, 34, 2168–2194, 1997.
[5] L. Pareschi and G. Russo. Asymptotic preserving Monte-Carlo methods for the Boltzmann equation. *Transp. Theo. Stat. Phys.*, 29, 415–430, 2000.
[6] L. Pareschi and G. Russo. Time Relaxed Monte Carlo methods for the Boltzmann equation. *SIAM J. Sci. Comp.*, 2000. submitted.
[7] D.I. Pullin. Direct simulation methods for compressible inviscid ideal gas flow. *Journal of Computational Physics*, 1978.
[8] R. Roveda, D.B. Goldstein, and P.L. Varghese Hybrid Euler/Direct Simulation Monte Carlo calculation of unsteady sit flow. *preprint*, 2000.

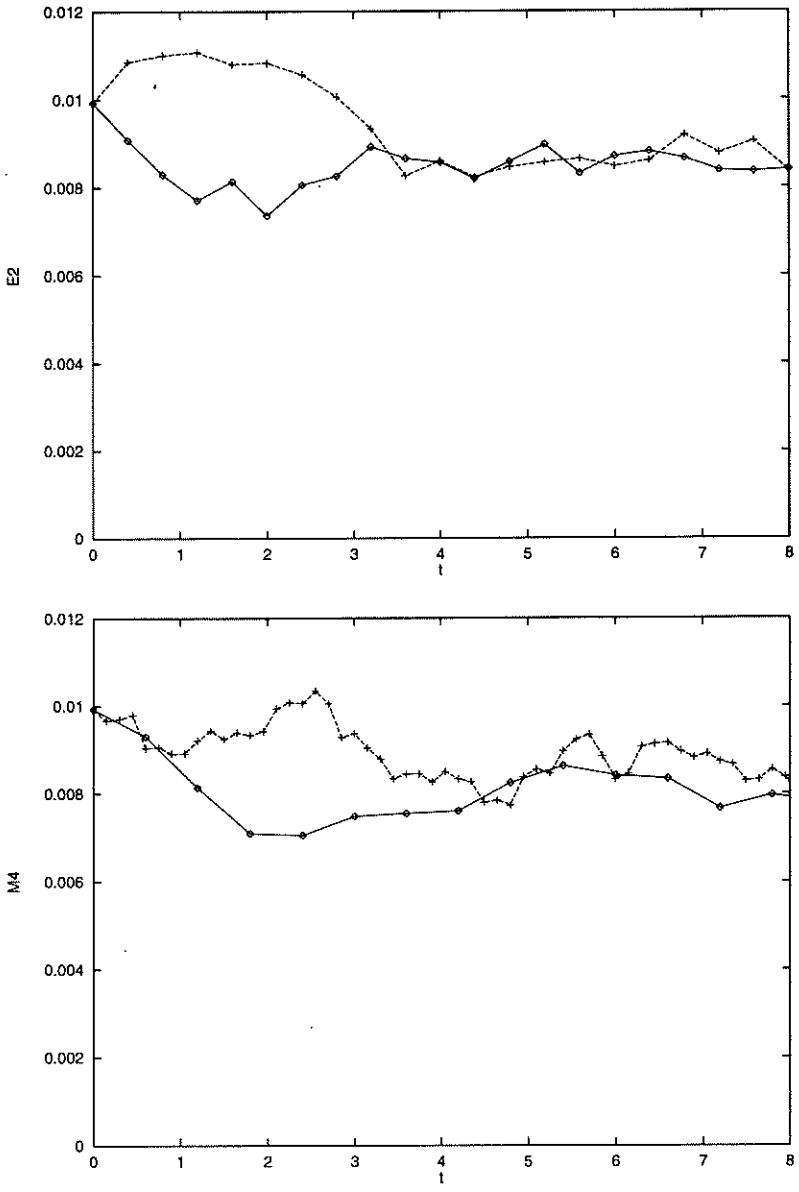

FIG. 6.1. Maxwell molecules: L^2 norm of the error vs time. DSMC (+) and TRMCH ($\diamond$). Top: $\Delta t = 0.4$. Bottom: $\Delta t = 0.15$ (DSMC), $\Delta t = 0.6$ (TRMCH).

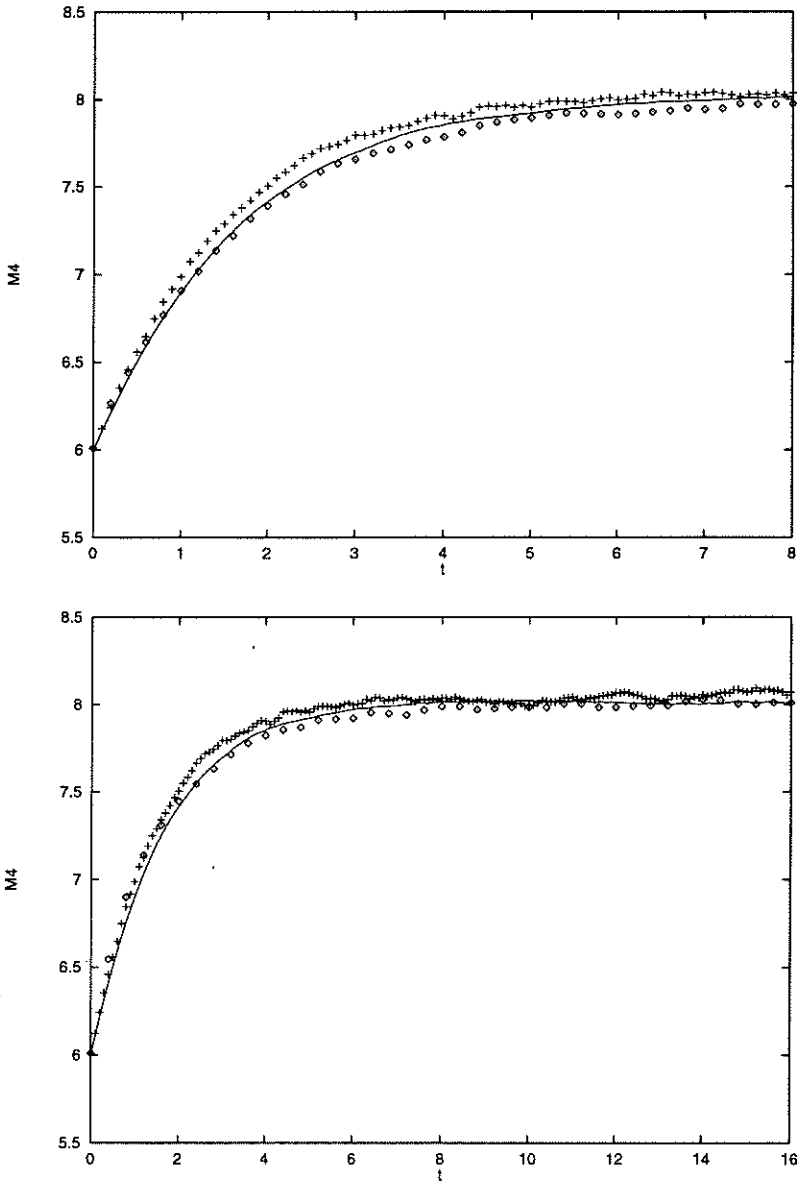

FIG. 6.2. Hard Sphere molecules: fourth order moment vs time. DSMC (+), TRMCH ($\diamond$), and "exact" (line) solution. Top: $\Delta t = 0.1$ for DSMC and $\Delta t = 0.2$ for TRMCH. Bottom: $\Delta t = 0.1$ for DSMC and $\Delta t = 0.4$ for TRMCH.

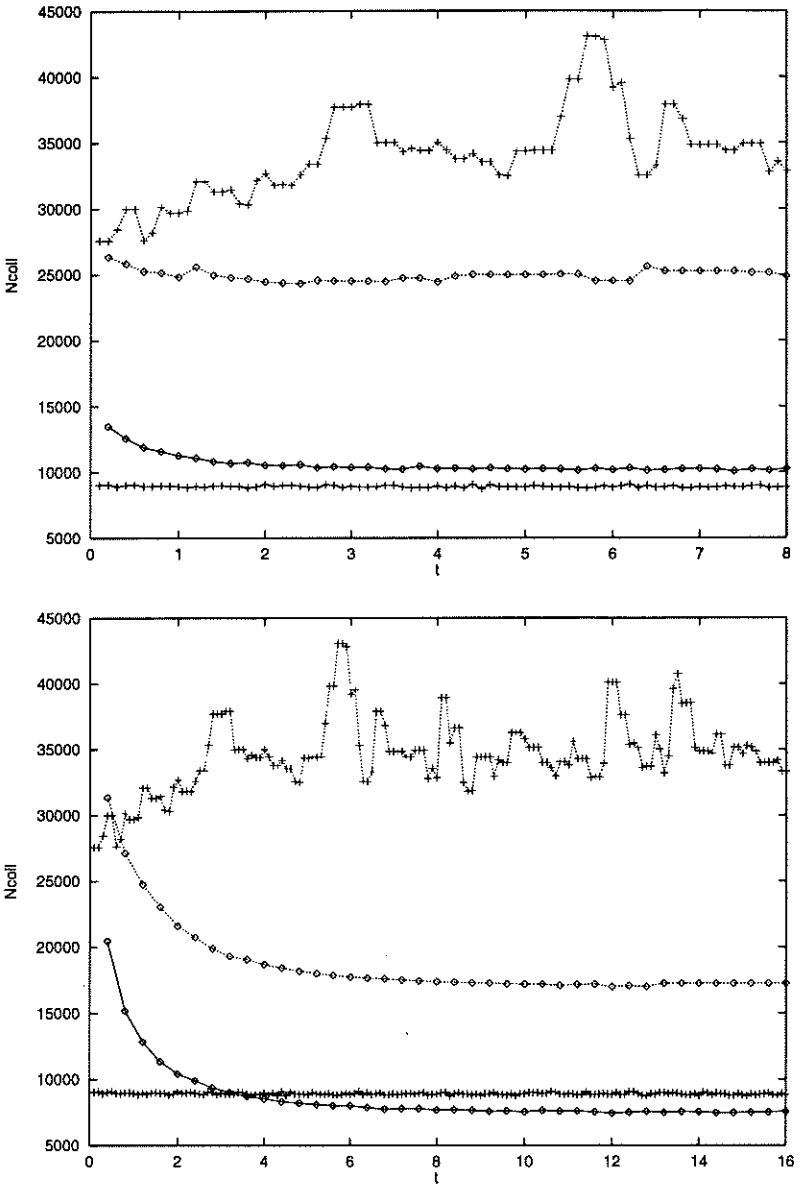

FIG. 6.3. Hard Sphere molecules: number of effective (line) and dummy (dashed line) collisions vs. time. DSMC (+), TRMCH (◇). Top: $\Delta t = 0.1$ for DSMC and $\Delta t = 0.2$ for TRMCH. Bottom: $\Delta t = 0.1$ for DSMC and $\Delta t = 0.4$ for TRMCH.

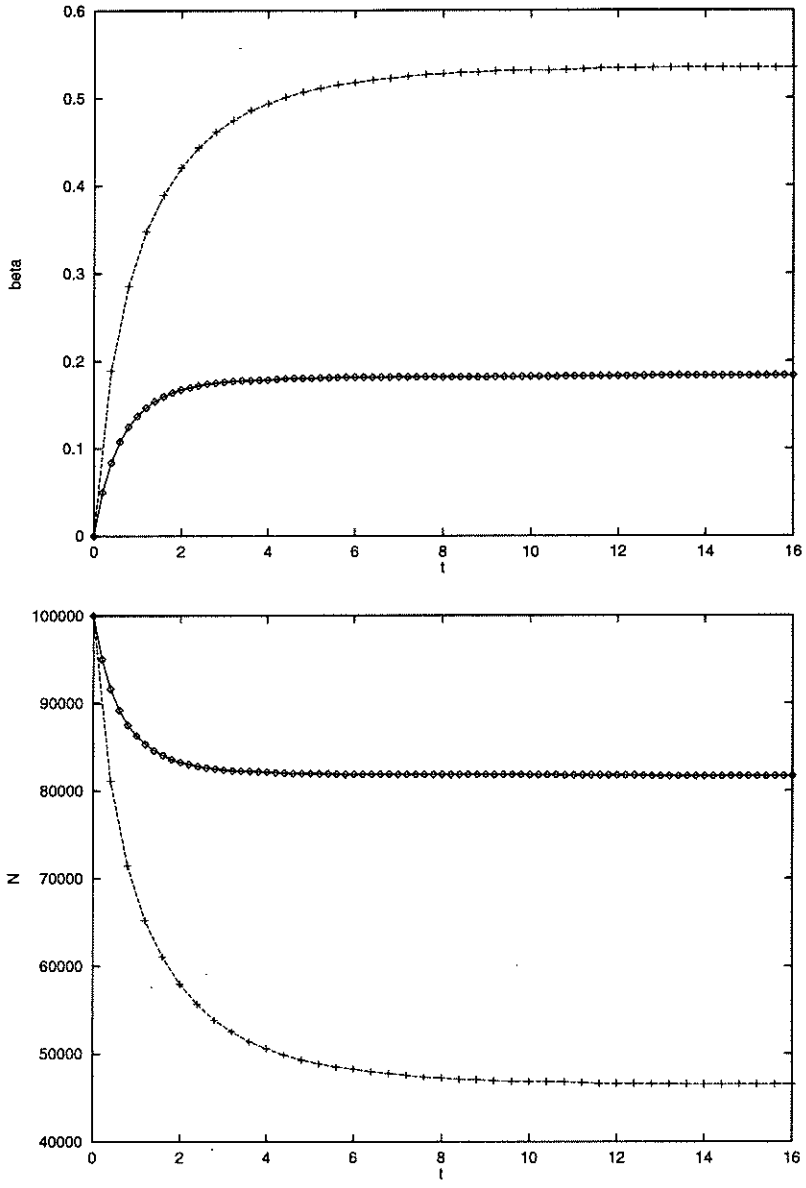

FIG. 6.4. Hard Sphere molecules: value of β^n (top) and number of particles (bottom) vs time for TRMCH. Time step: $\Delta t = 0.2$ ($\diamond$), $\Delta t = 0.4$ (+).